



Received: April 26, 2021
Revised: June 1, 2021
Accepted: June 21, 2021

Correspondence to:

Koung Mi Kang, M.D., Ph.D.
Department of Radiology, Seoul
National University College
of Medicine, Seoul National
University Hospital, 101 Daehak-
ro, Chongno-gu, Seoul 03080,
Korea.

Tel. +82-2-2072-3696

Fax. +82-2-743-6385

E-mail: we3001@gmail.com

This is an Open Access article distributed under the terms of the Creative Commons Attribution Non-Commercial License (<http://creativecommons.org/licenses/by-nc/4.0/>) which permits unrestricted non-commercial use, distribution, and reproduction in any medium, provided the original work is properly cited.

Copyright © 2021 Korean Society of Magnetic Resonance in Medicine (KSMRM)

Assessment of Mild Cognitive Impairment in Elderly Subjects Using a Fully Automated Brain Segmentation Software

Chiheon Kwon¹, Koung Mi Kang^{1,2}, Min Soo Byun³, Dahyun Yi⁴, Huijin Song⁵, Ji Ye Lee¹, Inpyeong Hwang¹, Roh-Eul Yoo¹, Tae Jin Yun¹, Seung Hong Choi^{1,2}, Ji-hoon Kim¹, Chul-Ho Sohn^{1,2}, Dong Young Lee^{6,7}, for the KBASE Research Group

¹Department of Radiology, Seoul National University Hospital, Seoul, Korea

²Department of Radiology, Seoul National University College of Medicine, Seoul, Korea

³Department of Psychiatry, Pusan National University Yangsan Hospital, Yangsan, Korea

⁴Institute of Human Behavioral Medicine, Seoul National University Medical Research Center, Seoul, Korea

⁵Biomedical Research Institute, Seoul National University Hospital, Seoul, Korea

⁶Department of Neuropsychiatry, Seoul National University Hospital, Seoul, Korea

⁷Department of Neuropsychiatry, Seoul National University College of Medicine, Seoul, Korea

Purpose: Mild cognitive impairment (MCI) is a prodromal stage of Alzheimer's disease (AD). Brain atrophy in this disease spectrum begins in the medial temporal lobe structure, which can be recognized by magnetic resonance imaging. To overcome the unsatisfactory inter-observer reliability of visual evaluation, quantitative brain volumetry has been developed and widely investigated for the diagnosis of MCI and AD. The aim of this study was to assess the prediction accuracy of quantitative brain volumetry using a fully automated segmentation software package, NeuroQuant®, for the diagnosis of MCI.

Materials and Methods: A total of 418 subjects from the Korean Brain Aging Study for Early Diagnosis and Prediction of Alzheimer's Disease cohort were included in our study. Each participant was allocated to either a cognitively normal old group (n = 285) or an MCI group (n = 133). Brain volumetric data were obtained from T1-weighted images using the NeuroQuant software package. Logistic regression and receiver operating characteristic (ROC) curve analyses were performed to investigate relevant brain regions and their prediction accuracies.

Results: Multivariate logistic regression analysis revealed that normative percentiles of the hippocampus (P < 0.001), amygdala (P = 0.003), frontal lobe (P = 0.049), medial parietal lobe (P = 0.023), and third ventricle (P = 0.012) were independent predictive factors for MCI. In ROC analysis, normative percentiles of the hippocampus and amygdala showed fair accuracies in the diagnosis of MCI (area under the curve: 0.739 and 0.727, respectively).

Conclusion: Normative percentiles of the hippocampus and amygdala provided by the fully automated segmentation software could be used for screening MCI with a reasonable post-processing time. This information might help us interpret structural MRI in patients with cognitive impairment.

Keywords: Automated brain segmentation; Magnetic resonance imaging; Mild cognitive impairment

INTRODUCTION

Mild cognitive impairment (MCI) refers to a decline in cognitive function with preserved normal daily activity. It is regarded as an intermediate disease entity between normal aging and Alzheimer's disease (AD), a major cause of dementia (1, 2). Neurodegeneration and consequent parenchymal atrophy in AD are most distinctive in the medial temporal lobe, a core structure in the pathogenesis of AD (3, 4). In the early stage, deposition of neurofibrillary tangle, one of hallmarks of AD pathophysiology, begins at the entorhinal cortex and extends into the hippocampus, amygdala, and parahippocampal gyrus (3-5). As the disease progresses, other brain regions are affected with the distribution of neurofibrillary tangles (3, 6-8). Morphological changes on magnetic resonance imaging (MRI) also follow the progression of neurofibrillary tangles (9, 10). In the understanding of this patterned neurodegeneration, brain volume analysis has a value in early diagnosis and monitoring of AD spectrum.

However, qualitative assessment of brain atrophy is limited due to an unsatisfactory inter-observer reliability. Previous studies have reported that the inter-observer agreement ranges from 40% to 70% in visual evaluation of medial temporal lobe atrophy on MR images (3, 11, 12). Moreover, the inter-rater reliability is significantly decreased in less experienced observers (13). Accordingly, the need for quantitative volumetric measures with a clinically acceptable reproducibility has been emphasized.

Several fully automated segmentation software packages including FSL, FreeSurfer, and SPM have been developed for research purposes, although their labor-intensive nature and long processing time impede their clinical applications (14). To improve accessibility and practicality, various software tools designed for routine clinical practice have been marketed. Among them, NeuroQuant® (CorTechs Labs, San Diego, CA, USA) first approved by the United States Food and Drug Administration in 2006 has become one of the most frequently used clinically oriented automated segmentation software (15, 16). With its application, absolute volume data of various brain regions, relative volumes after correcting head size, and age- and gender-matched normative percentiles can be obtained in 6-8 min. The purpose of this study was to validate the efficacy of NeuroQuant in the differential diagnosis of normal old and MCI patients essential for early detection and management of the AD spectrum. The diagnosis of MCI could help clinicians counsel their patients to prepare possible

neurocognitive deterioration and to prevent detrimental effects caused by physical and psychological dysfunctions. To achieve the purpose of this study, prediction accuracies of normative volumes of medial temporal lobe structures in the assessment of MCI were evaluated and compared with those of previous reports. Diagnostic performances of other brain structures were also assessed.

MATERIALS AND METHODS

Study Population

The study population was derived from the Korean Brain Aging Study for the Early Diagnosis and Prediction of Alzheimer's Disease (KBASE) cohort (17). In this ongoing cohort study, subjects have been prospectively recruited since 2014 for the identification of novel biomarkers for early diagnosis of AD. They were classified into four groups: cognitively normal young and middle-aged (age of 20-54 years, CN-young), cognitively normal old (age of 55-90 years, CN-old), mild cognitive impairment (MCI), and AD. Among them, CN-old group (n = 285) and MCI group (n = 133) of individuals (total, n = 418) were included in our study. The MCI group was defined as those aged 55-90 years who demonstrated subjective and objective memory impairments without difficulty in other functional activities. The diagnosis was determined by a consensus panel comprising board-certified psychiatrists, clinical neuropsychologists, and psychometrists. Exclusion criteria were as follows: (a) major mental disorders; (b) neurological or medical condition degrading cognitive function; (c) MR-contraindicated status; (d) illiteracy; (e) visual/hearing impairment complicating communication and clinical interview; (f) investigational medication; and (g) pregnancy or breastfeeding. Details of our inclusion and exclusion criteria are available in a previous report on KBASE cohort recruitment (17). This study and the precedent cohort study were approved by our Institutional Review Board.

Diagnosis of MCI

Following the National Institute of Aging and Alzheimer's Association guidelines, individuals with the following inclusion criteria were allocated to the MCI group: (a) subjective or objective memory complaints, (b) decreased memory function for age, gender, and education; (c) no impairment in daily activity; and (d) no dementia. Objective memory decline was assessed using a systematized test battery mainly based on the Korean version of the

Consortium to Establish a Registry for Alzheimer's Disease Assessment Packet. Neurological and physical examinations were performed by clinicians.

Image Acquisition

Simultaneous acquisition of 11C-Pittsburgh compound B-positron emission tomography (PET) and MR images was performed using a hybrid PET-MR system (3.0T Biograph mMR, Siemens, Munich, Germany) in accordance with the manufacturer's guidelines. MR imaging included three-dimensional (3D)-T1-weighted magnetization-prepared rapid acquisition with gradient echo (MPRAGE) sequence scans obtained in sagittal orientation. The following parameters were used for 3D T1-weighted images: repetition time = 1670 ms, echo time = 1.89 ms, field of view = 250 mm, matrix size = 256 × 256, and slice thickness = 1.0 mm.

MR-Based Volumetric Analyses

Brain volumetric data for each subject were obtained from T1-weighted MPRAGE sequence images using the NeuroQuant software package that could automatically process images with algorithms including quality assurance, gradient inhomogeneity correction, field inhomogeneity adjustment, skull stripping, and automatic segmentation (18). The software then provided volumetric data for each segmented structure, including absolute volume, head-size-corrected volume (volume percentage of intracranial volume [ICV]), and normative percentile. As normative percentiles were calculated in comparison with an age- and sex-matched healthy control population, we focused on them to take into account age and sex of subjects. The sum of right and left volumes was utilized for structures with bilaterality.

Statistical Analysis

We compared volumetric differences between CN-old and MCI groups for all brain regions provided by the NeuroQuant software. Among all segmented brain regions, medial temporal lobe structures known to be key elements during early neuropathogenesis of AD were primarily focused, although all brain structures were included in the following statistical analysis. In univariable analysis, either a two-sample t-test or a Welch's t-test was applied for variables with equal or unequal variance, respectively. Variance equality was assessed using Levene's test. Variables with $P < 0.05$ were included in the subsequent multivariate analysis. A multivariable backward logistic regression model was used to identify independent predictive factors

of MCI and statistically significant variables were selected as predictors. Statistical significance was set at $P < 0.05$. Receiver operating characteristic (ROC) curve analyses were performed for those variables. Area under the curve (AUC) was used to estimate the prediction accuracy as follows: excellent (0.9–1.0), good (0.8–0.9), fair (0.7–0.8), and poor (0.6–0.7) (19). All statistical analyses were performed using SPSS 25 software (IBM, Armonk, New York, NY, USA).

RESULTS

Baseline Characteristics

In our study population, 285 cognitively normal old (CN-old, mean age of 69.1 ± 8.1 years) and 133 MCI (mean age of 73.5 ± 6.9 years) subjects were included. Male to female ratios were 1:1.07 and 1:1.89 in CN-old and MCI groups, respectively. Age, sex, and level of education demonstrated statistically significant differences between the two groups (all P -values < 0.05). Education level was considered in the cognitive function test battery. Detailed demographic data are presented in Table 1.

Medial Temporal Lobe Structures in the MCI Group

The NeuroQuant software provided volumetric data for 71 segmental structures. Detailed results for each brain region are presented in Supplementary Table 1. Regarding medial temporal lobe structures, mean and standard deviations of normative percentiles of the hippocampus, amygdala, entorhinal cortex, and parahippocampal gyrus were $72.4 \pm 26.6\%$, $73.5 \pm 25.3\%$, $62.2 \pm 31.7\%$, and $48.6 \pm 27.6\%$, respectively, in the CN-old group. They were $42.7 \pm 35.6\%$, $46.5 \pm 34.6\%$, $44.8 \pm 34.1\%$, and $41.3 \pm 28.8\%$, respectively, in the MCI group. Normative percentiles of

Table 1. Demographic Information of the Study Population

	All	CN-old	MCI	P-value
Number of subjects (n)	418	285	133	
Age (years)	70.5 ± 8.0	69.1 ± 8.1	73.5 ± 6.9	< 0.001
Sex (n)				0.008
Male	184	138	46	
Female	234	147	87	
Education (years)	11.2 ± 4.8	11.8 ± 4.8	10.0 ± 4.6	< 0.001

Data for years are presented as mean \pm standard deviation. P-values are results of univariate analysis. Data were analyzed either by two-sample t-test for continuous variables or chi-square test for categorical variables.

CN-old = cognitively normal old; MCI = mild cognitive impairment

all these structures demonstrated statistically significant differences between CN-old and MCI groups ($P < 0.001$ for the hippocampus, amygdala, and entorhinal cortex; $P = 0.013$ for the parahippocampal gyrus) (Table 2). Mean normative percentiles of the inferior lateral ventricle were significantly different between the CN-old group ($60.7 \pm 26.4\%$) and the MCI group ($75.4 \pm 23.9\%$) ($P < 0.001$) (Table 2).

Independent Predicting Factors and Accuracy

Among 71 segmental structures, normative percentiles of 67 brain regions were included in the univariate analysis. Four structures (corpus callosum, inferior lateral ventricle choroid plexus, superior lateral ventricle choroid plexus, and 5th ventricle) were not included since their normative percentiles were not provided by the NeuroQuant software. Univariate analysis revealed that normative percentiles of the 36 brain regions were statistically different between

CN-old and MCI groups ($P < 0.05$). Detailed list and their P-values are described in Supplementary Table 1. All these 36 structures were included in the subsequent multivariate backward logistic regression analysis. Normative percentiles of the following five anatomical structures were independent predicting factors for MCI: hippocampus ($P < 0.001$), amygdala ($P = 0.003$), frontal lobe ($P = 0.049$), medial parietal lobes ($P = 0.023$), and third ventricle ($P = 0.012$) (Table 3).

In ROC analysis, among all segmented structures, the hippocampus and amygdala had AUC larger than 0.7, indicating a fair degree of diagnostic performance. With a cut-off value of less than 51.5%, the hippocampal volume could predict MCI with a sensitivity of 60.2% and a specificity of 80.0% (AUC: 0.739, 95% confidence interval [CI]: 0.685-0.794). The volume of the amygdala showed comparable accuracy, with a sensitivity of 48.9% and a

Table 2. Volumetric Data for Medial Temporal Lobe Structures and the Inferior Lateral Ventricle

	All	CN-old	MCI	P-value
Hippocampus				
Volume (cm ³)	6.78 (1.15)	7.13 (1.00)	6.04 (1.10)	< 0.001
% ICV	0.460 (0.075)	0.480 (0.064)	0.418 (0.080)	< 0.001
Normative percentile (%)	63.0 (32.8)	72.4 (26.6)	42.7 (35.6)	< 0.001
Amygdala				
Volume (cm ³)	2.99 (0.48)	3.13 (0.42)	2.70 (0.47)	< 0.001
% ICV	0.202 (0.029)	0.210 (0.025)	0.186 (0.031)	< 0.001
Normative percentile (%)	64.9 (31.2)	73.5 (25.3)	46.5 (34.6)	< 0.001
Entorhinal cortex				
Volume (cm ³)	5.45 (1.20)	5.71 (1.16)	4.90 (1.09)	< 0.001
% ICV	0.367 (0.069)	0.382 (0.065)	0.337 (0.068)	< 0.001
Normative percentile (%)	56.6 (33.5)	62.2 (31.7)	44.8 (34.1)	< 0.001
Parahippocampal gyrus				
Volume (cm ³)	4.38 (0.71)	4.48 (0.69)	4.15 (0.70)	< 0.001
% ICV	0.295 (0.034)	0.300 (0.031)	0.286 (0.039)	< 0.001
Normative percentile (%)	46.3 (28.2)	48.6 (27.6)	41.3 (28.8)	0.013
Inferior lateral ventricle				
Volume (cm ³)	2.61 (1.36)	2.36 (1.23)	3.14 (1.47)	< 0.001
% ICV	0.18 (0.09)	0.16 (0.08)	0.21 (0.09)	< 0.001
Normative percentile (%)	65.4 (26.5)	60.7 (26.4)	75.4 (23.9)	< 0.001

Unless otherwise specified, data are presented as average values with standard deviations in parentheses. P-values are results of univariate analysis comparing CN-old and MCI groups. They were calculated either by the Welch t-test for the hippocampus, amygdala, and inferior lateral ventricle or two-sample t-test for the entorhinal cortex and parahippocampal gyrus. % ICV is the absolute volume divided by intracranial volume

% ICV = percentage of intracranial volume; CN-old = cognitively normal old; MCI = mild cognitive impairment

specificity of 86.0% (AUC: 0.727, 95% CI: 0.673-0.781) at a cut-off value of 41.5 percentile (Fig. 1). However, other medial temporal lobe structures, entorhinal cortex, and parahippocampal gyrus showed unsatisfactory predictive accuracies. AUCs for the entorhinal cortex and the parahippocampal gyrus were 0.649 (95% CI: 0.591-0.706) and 0.578 (95% CI: 0.518-0.638), respectively. Diagnostic performances of other independent predictive variables (the frontal lobe, medial temporal lobe, and third ventricle) were also poor (AUC < 0.7) (Table 3).

DISCUSSION

In this study, we assessed the value of quantitative brain volumetry using a commercially available, fully automated segmentation software package for the diagnosis of MCI. Normative percentiles of the hippocampus and amygdala demonstrated fair prediction accuracies for MCI (AUC: 0.7-0.8). This result was similar to those of previous reports (20-22), in which segmentation was performed either manually or with labor-intensive, research-oriented software algorithms such as SPM and FreeSurfer. Considering the short processing time (6-8 min) and the straightforward

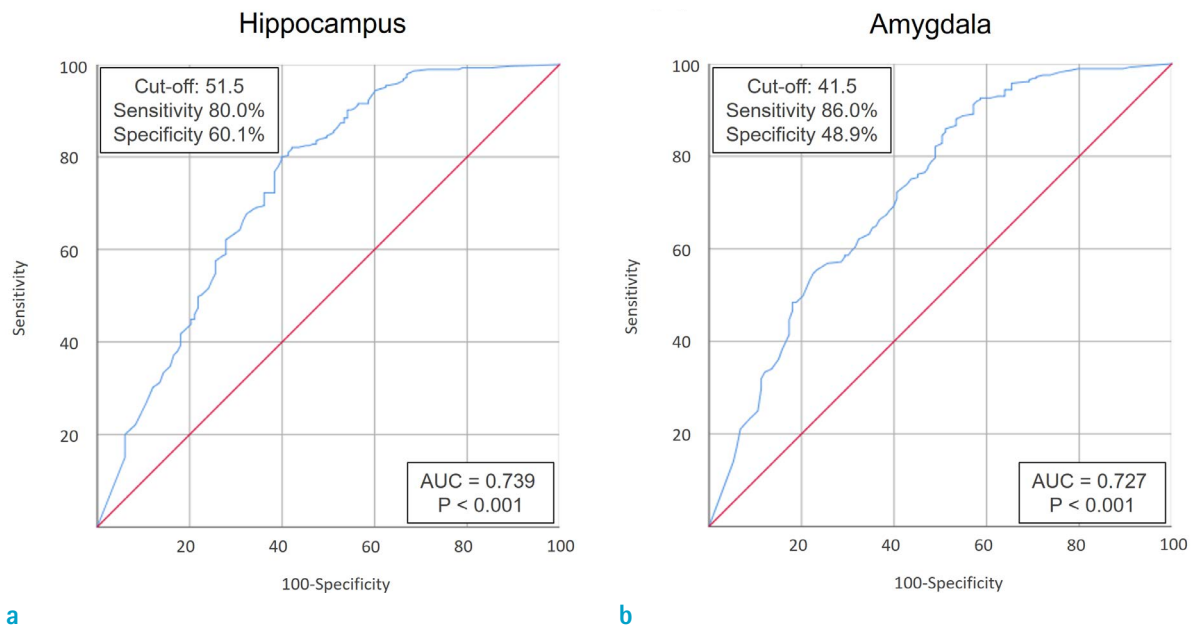


Fig. 1. ROC Curves for the hippocampus and amygdala. ROC analyses were performed for normative percentiles of the hippocampus (a) and amygdala (b) comparing CN-old and MCI groups. The cut-off value was determined using the Youden method. Sensitivity and specificity were calculated at the cut-off. AUC = area under the curve; CN-old = cognitively normal old; MCI = mild cognitive impairment; ROC = receiver operating characteristic

Table 3. Results of Multivariate Logistic Regression and ROC Analyses

	P-value	OR	95% CI for OR	AUC	95% CI for AUC
Hippocampus	< 0.001	0.974	0.963, 0.985	0.739	0.685, 0.794
Amygdala	0.003	0.985	0.975, 0.995	0.727	0.673, 0.781
Frontal lobe	0.049	0.983	0.996, 1.000	0.600	0.539, 0.662
Medial parietal lobe	0.023	0.986	0.973, 0.997	0.591	0.531, 0.561
Third ventricle	0.012	1.012	1.002, 1.023	0.655	0.600, 0.710

Data shown here are independent predictive factors for MCI. P-values and odds ratios are results of multivariate backward logistic regression analysis. Both multivariate and ROC analyses were performed using the normative percentile volume of each brain structure.

AUC = area under the curve; CI = confidence interval; MCI = mild cognitive impairment; OR = odds ratio; ROC = receiver operating characteristic

accessibility, NeuroQuant could be more useful in an actual clinical setting which requires visualized volumetric report within each consultation session.

NeuroQuant has been extensively investigated in the AD spectrum. Persson et al. (23) have compared the hippocampal volume between MCI and AD groups. They demonstrated that it had a good accuracy (AUC: 0.88, 95% CI: 0.78–0.97) for discriminating AD from subjective and mild cognitive impairment. Ferrari et al. (24) have reported an unsatisfactory prediction performance of hippocampal volume when comparing AD/high-risk MCI to low-risk MCI (AUC: 0.65, 95% CI: 0.49–0.87). England et al. (25) have evaluated volumetric differences in the hippocampus and inferior lateral ventricle between 43 healthy old and 57 MCI subjects (72.1% sensitivity and 61.4% specificity with discrimination function). Our study similarly validated this software tool for the diagnosis of MCI among non-demented subjects. It could be distinguished from prior studies by utilizing a prospectively recruited cohort and a relatively larger population. In addition, we focused on age- and gender-matched normative percentiles rather than the absolute volume and the percentage of ICV primarily analyzed in previous studies. Our results also demonstrated the potential clinical usefulness in a different ethnic group, Korean population, compared to previous works.

Several studies have also demonstrated the efficacy of NeuroQuant in the risk stratification of patients with MCI. Tanpitukpongse et al. (26) have assessed its predictive utility in the estimation of MCI-to-AD conversion within 3 years. The hippocampal volume was predictive of AD conversion in patients with MCI (AUC: 0.69, 95% CI: 0.61–0.76) (26). Kang et al. (14) have demonstrated the performance of normative hippocampal volume in the prediction of amyloid beta positivity in MCI subjects (AUC: 0.72, 95% CI: 0.64–0.80).

The pathogenesis of AD affects the medial temporal lobe, including the entorhinal cortex, hippocampus, amygdala, and parahippocampus (3, 4). The entorhinal cortex is the structure in which the accumulation of neurofibrillary tangles begins. Accordingly, regional brain atrophy was first observed in the entorhinal cortex even before the onset of symptoms, namely preclinical AD (27). In our study, the diagnostic performance of entorhinal atrophy was unsatisfactory. This might be partly attributable to asymptomatic preclinical AD subjects allocated to the cognitively normal old group.

Diagnostic performances of normative percentiles of the hippocampus and amygdala atrophy were fair. This might be attributable to the use of baseline data derived from

a single time point rather than a longitudinal volumetric change. The decline in brain volume is faster in MCI and AD patients than in normal aging (28). The rate of atrophy accelerates as the disease progresses (28–30). Collective volumetric analysis with serial follow-up images may lead to a better diagnostic accuracy. However, initial estimation with baseline data at the time of presentation is also valuable for early detection of the AD spectrum.

As a secondary change to adjacent parenchymal atrophy, dilatation of ventricular structures can be observed in the spectrum of AD (31). Previous reports have suggested that lateral ventricular enlargement is a promising biomarker for discriminating between normal elderly and MCI patients (31–33). In particular, an increase in the inferior lateral ventricle has been pronounced as a result of medial temporal lobe structural shrinkage (25, 34, 35). In our study, the inferior lateral ventricle, superior lateral ventricle, and third ventricle demonstrated statistically significant enlargements in the MCI group compared to the CN-old group, although their prediction accuracies were poor (AUC: 0.5–0.7).

Our study had several limitations. First, this was a single-center study. An identical MRI machine with the same imaging protocol was applied to all subjects. Therefore, intra-scan and inter-scan variabilities could not be evaluated. They require further validation through future studies to improve clinical practicality. Second, despite a generally excellent correlation between NeuroQuant and labor-intensive segmentation modalities, several anatomic structures such as the pallidum and cerebellar white matter have been reported to have poor inter-method reliabilities (14, 15). However, they are not known to be significant in the earlier neuropathology of the AD spectrum. Third, structural differences derived from ethnicity could affect the accuracy of automated segmentation. Normative population data installed in the NeuroQuant could have discrepancies for the Korean population used in our study (34, 36). However, considering that normative percentiles, even relative to a disparate population, demonstrated fair diagnostic performances, better outcomes could be expected for future studies using a more targeted normative database, such as the Korean norm for our cohort.

In conclusion, normative percentiles of the hippocampus and amygdala obtained from NeuroQuant could be used for the diagnosis of MCI. With the merit of its acceptable accessibility and reproducibility, NeuroQuant could be used by clinicians to obtain additional information for discriminating MCI patients from normal aging ones, which

can be beneficial for early diagnosis and management of the AD spectrum.

Supplementary Materials

The Table Supplement is available with this article at <https://doi.org/10.13104/imri.2021.25.3.164>

Acknowledgments

This study was supported by a Scientific Research Fund of the Korean Society of Magnetic Resonance in Medicine (Grant no. 06-20191860) and a SNUH Research Fund (Grant no. 04-20190500). This work was also supported by a Korea Medical Device Development Fund grant funded by the Korea government (the Ministry of Science and ICT, the Ministry of Trade, Industry and Energy, the Ministry of Health & Welfare, the Ministry of Food and Drug Safety) (Project Number: KMDF_PR_20200901_0062, 9991006735).

REFERENCES

- Petersen RC. Mild cognitive impairment. *Continuum (Minneapolis)* 2016;22:404-418
- Jongsiriyanyong S, Limpawattana P. Mild cognitive impairment in clinical practice: a review article. *Am J Alzheimers Dis Other Demen* 2018;33:500-507
- Rathakrishnan BG, Doraiswamy PM, Petrella JR. Science to practice: translating automated brain MRI volumetry in Alzheimer's disease from research to routine diagnostic use in the work-up of dementia. *Front Neurol* 2014;4:216
- Braak E, Griffling K, Arai K, Bohl J, Bratzke H, Braak H. Neuropathology of Alzheimer's disease: what is new since A. Alzheimer? *Eur Arch Psychiatry Clin Neurosci* 1999;249 Suppl 3:14-22
- Killiany RJ, Hyman BT, Gomez-Isla T, et al. MRI measures of entorhinal cortex vs hippocampus in preclinical AD. *Neurology* 2002;58:1188-1196
- Bondi MW, Edmonds EC, Salmon DP. Alzheimer's disease: past, present, and future. *J Int Neuropsychol Soc* 2017;23:818-831
- Lane CA, Hardy J, Schott JM. Alzheimer's disease. *Eur J Neurol* 2018;25:59-70
- Ballard C, Gauthier S, Corbett A, Brayne C, Aarsland D, Jones E. Alzheimer's disease. *Lancet* 2011;377:1019-1031
- Whitwell JL. Progression of atrophy in Alzheimer's disease and related disorders. *Neurotox Res* 2010;18:339-346
- Whitwell JL, Josephs KA, Murray ME, et al. MRI correlates of neurofibrillary tangle pathology at autopsy: a voxel-based morphometry study. *Neurology* 2008;71:743-749
- Scheltens P, Launer LJ, Barkhof F, Weinstein HC, van Gool WA. Visual assessment of medial temporal lobe atrophy on magnetic resonance imaging: interobserver reliability. *J Neurol* 1995;242:557-560
- Pasquier F, Leys D, Weerts JG, Mounier-Vehier F, Barkhof F, Scheltens P. Inter- and intraobserver reproducibility of cerebral atrophy assessment on MRI scans with hemispheric infarcts. *Eur Neurol* 1996;36:268-272
- Cavallin L, Loken K, Engedal K, et al. Overtime reliability of medial temporal lobe atrophy rating in a clinical setting. *Acta Radiol* 2012;53:318-323
- Kang KM, Sohn CH, Byun MS, et al. Prediction of amyloid positivity in mild cognitive impairment using fully automated brain segmentation software. *Neuropsychiatr Dis Treat* 2020;16:1745-1754
- Ochs AL, Ross DE, Zannoni MD, Abildskov TJ, Bigler ED, Alzheimer's Disease Neuroimaging Initiative. Comparison of automated brain volume measures obtained with NeuroQuant and FreeSurfer. *J Neuroimaging* 2015;25:721-727
- Chung JH, Park HJ, Kim KT. Scoliosis after pectus excavatum correction: does it improve or worsen? *Eur J Cardiothorac Surg* 2017;52:76-82
- Byun MS, Yi D, Lee JH, et al. Korean brain aging study for the early diagnosis and prediction of Alzheimer's disease: methodology and baseline sample characteristics. *Psychiatry Investig* 2017;14:851-863
- Brewer JB, Magda S, Airriess C, Smith ME. Fully-automated quantification of regional brain volumes for improved detection of focal atrophy in Alzheimer disease. *AJNR Am J Neuroradiol* 2009;30:578-580
- Carter JV, Pan J, Rai SN, Galandiuk S. ROC-ing along: evaluation and interpretation of receiver operating characteristic curves. *Surgery* 2016;159:1638-1645
- Mueller SG, Schuff N, Yaffe K, Madison C, Miller B, Weiner MW. Hippocampal atrophy patterns in mild cognitive impairment and Alzheimer's disease. *Hum Brain Mapp* 2010;31:1339-1347
- Visser PJ, Scheltens P, Verhey FR, et al. Medial temporal lobe atrophy and memory dysfunction as predictors for dementia in subjects with mild cognitive impairment. *J Neurol* 1999;246:477-485
- Pini L, Pievani M, Bocchetta M, et al. Brain atrophy in Alzheimer's disease and aging. *Ageing Res Rev* 2016;30:25-48
- Persson K, Barca ML, Cavallin L, et al. Comparison of automated volumetry of the hippocampus using NeuroQuant(R) and visual assessment of the medial temporal lobe in Alzheimer's disease. *Acta Radiol* 2018;59:997-1001

24. Ferrari BL, Neto GCC, Nucci MP, et al. The accuracy of hippocampal volumetry and glucose metabolism for the diagnosis of patients with suspected Alzheimer's disease, using automatic quantitative clinical tools. *Medicine (Baltimore)* 2019;98:e17824
25. England HB, Gillis MM, Hampstead BM. RBANS memory indices are related to medial temporal lobe volumetrics in healthy older adults and those with mild cognitive impairment. *Arch Clin Neuropsychol* 2014;29:322-328
26. Tanpitukpongse TP, Mazurowski MA, Ikkena J, Petrella JR, Alzheimer's Disease Neuroimaging Initiative. Predictive utility of marketed volumetric software tools in subjects at risk for Alzheimer disease: do regions outside the hippocampus matter? *AJNR Am J Neuroradiol* 2017;38:546-552
27. Kulason S, Xu E, Tward DJ, et al. Entorhinal and transentorhinal atrophy in preclinical Alzheimer's disease. *Front Neurosci* 2020;14:804
28. Tabatabaei-Jafari H, Shaw ME, Cherbuin N. Cerebral atrophy in mild cognitive impairment: a systematic review with meta-analysis. *Alzheimers Dement (Amst)* 2015;1:487-504
29. Sluimer JD, van der Flier WM, Karas GB, et al. Accelerating regional atrophy rates in the progression from normal aging to Alzheimer's disease. *Eur Radiol* 2009;19:2826-2833
30. Wang PN, Liu HC, Lirng JF, Lin KN, Wu ZA. Accelerated hippocampal atrophy rates in stable and progressive amnesic mild cognitive impairment. *Psychiatry Res* 2009;171:221-231
31. Apostolova LG, Green AE, Babakchanian S, et al. Hippocampal atrophy and ventricular enlargement in normal aging, mild cognitive impairment (MCI), and Alzheimer disease. *Alzheimer Dis Assoc Disord* 2012;26:17-27
32. Nestor SM, Rupsingh R, Borrie M, et al. Ventricular enlargement as a possible measure of Alzheimer's disease progression validated using the Alzheimer's disease neuroimaging initiative database. *Brain* 2008;131:2443-2454
33. Chou YY, Lepore N, Avedissian C, et al. Mapping correlations between ventricular expansion and CSF amyloid and tau biomarkers in 240 subjects with Alzheimer's disease, mild cognitive impairment and elderly controls. *Neuroimage* 2009;46:394-410
34. Min J, Moon WJ, Jeon JY, Choi JW, Moon YS, Han SH. Diagnostic efficacy of structural MRI in patients with mild-to-moderate Alzheimer disease: automated volumetric assessment versus visual assessment. *AJR Am J Roentgenol* 2017;208:617-623
35. Bartos A, Gregus D, Ibrahim I, Tintera J. Brain volumes and their ratios in Alzheimer's disease on magnetic resonance imaging segmented using Freesurfer 6.0. *Psychiatry Res Neuroimaging* 2019;287:70-74
36. Chee MW, Zheng H, Goh JO, Park D, Sutton BP. Brain structure in young and old East Asians and Westerners: comparisons of structural volume and cortical thickness. *J Cogn Neurosci* 2011;23:1065-1079